

# Microbiome-microglial crosstalk in graft-versus-host disease of the central nervous system

Sangya Chatterjee<sup>1,2</sup>, Janaki Manoj Vinnakota<sup>1,2</sup>, Daniel Erny<sup>3</sup>, Solveig Runge<sup>4</sup>, Stephan P Rosshart<sup>4</sup>, Geoffroy Andrieux<sup>5</sup>, Melanie Boerries<sup>5</sup>, Marco Prinz<sup>3,6,7</sup>, Robert Zeiser<sup>1,6,8</sup>

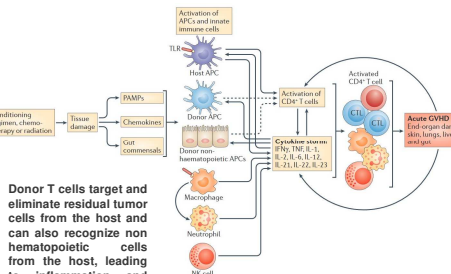
<sup>1</sup>Department of Medicine I - Medical centre - University of Freiburg, Faculty of Medicine, Freiburg, Germany  
<sup>2</sup>Faculty of Biology, Albert-Ludwigs-University, Freiburg, Germany  
<sup>3</sup>Institute for Neuropathology, Medical Faculty, University of Freiburg, Freiburg, Germany  
<sup>4</sup>Department of Medicine II - Medical centre - University of Freiburg, Faculty of Medicine, Freiburg, Germany  
<sup>5</sup>Institute of Medical Bioinformatics and Systems Medicine, Medical Center - University of Freiburg, Freiburg, Germany  
<sup>6</sup>Signaling Research Centres BIOS and CIBSS - Centre for Integrative Biological Signaling Studies, University of Freiburg, Freiburg, Germany  
<sup>7</sup>Center for NeuroModulation, Faculty of Medicine, University of Freiburg, Freiburg, Germany  
<sup>8</sup>German Cancer Consortium (DKTK), Partner Site Freiburg, and German Cancer Research Center (DKFZ), Heidelberg, Germany



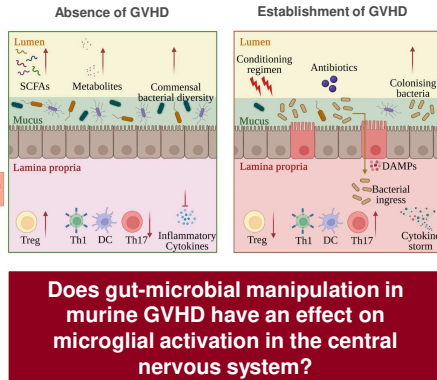
UNIVERSITÄT  
KLINIKUM FREIBURG

## Introduction

Allogeneic hematopoietic cell transplant (Allo-HCT) is a treatment modality for various hematological disorders. In patients, Graft-versus-host disease (GVHD) is the major clinical complication arising after Allo-HCT.



Adapted from Blazar BR et al. *Nature Reviews Immunology*, 2012



Does gut-microbial manipulation in murine GVHD have an effect on microglial activation in the central nervous system?

## Methods

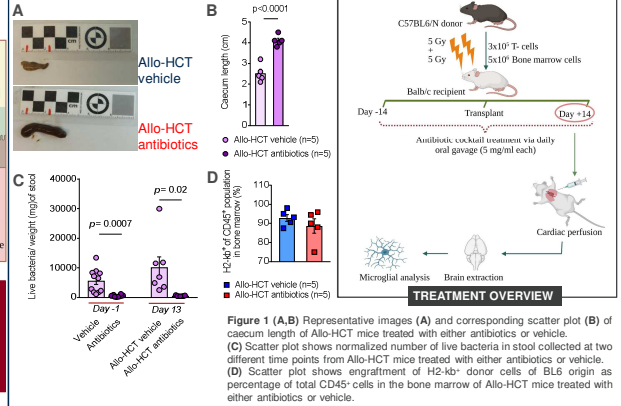


Figure 1 (A, B) Representative images (A) and corresponding scatter plot (B) of cecum length of Allo-HCT mice treated with either antibiotics or vehicle. (C) Scatter plot shows normalized number of live bacteria in stool collected at two different time points from Allo-HCT mice treated with either antibiotics or vehicle. (D) Scatter plot shows engraftment of H2-kg<sup>+</sup> donor cells of BL6 origin as percentage of total CD45<sup>+</sup> cells in the bone marrow of Allo-HCT mice treated with either antibiotics or vehicle.

## Microbiome depletion drives T-cell towards activation and pro-inflammatory phenotype

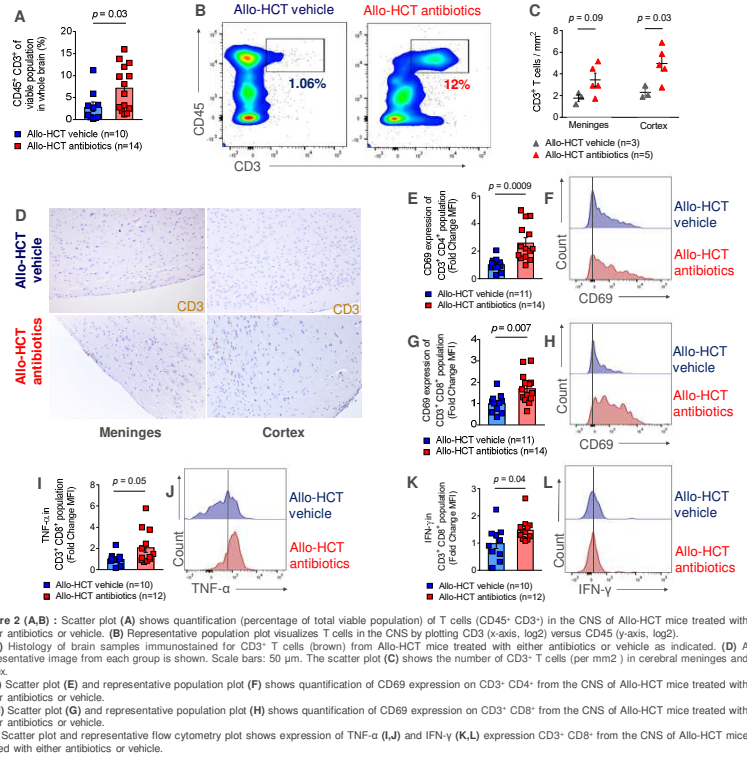


Figure 2 (A, B) Scatter plot (A) shows quantification (percentage of total viable population) of T cells (CD45<sup>+</sup> CD3<sup>+</sup>) in the CNS of Allo-HCT mice treated with either antibiotics or vehicle. (B) Representative population plot visualizes T cells in the CNS by plotting CD3 (x-axis, log<sub>2</sub>) versus CD45 (y-axis, log<sub>2</sub>). (C, D) Histology of brain samples immunostained for CD3<sup>+</sup> T cells (brown) from Allo-HCT mice treated with either antibiotics or vehicle as indicated. (D) A representative image from each group is shown. Scale bars: 50 μm. The scatter plot (C) shows the number of CD3<sup>+</sup> T cells (per mm<sup>2</sup>) in cerebral meninges and cortex. (E-F) Scatter plot (E) and representative population plot (F) shows quantification of CD69 expression on CD3<sup>+</sup> CD4<sup>+</sup> from the CNS of Allo-HCT mice treated with either antibiotics or vehicle. (G-H) Scatter plot (G) and representative population plot (H) shows quantification of CD69 expression on CD3<sup>+</sup> CD8<sup>+</sup> from the CNS of Allo-HCT mice treated with either antibiotics or vehicle. (I-L) Scatter plot and representative flow cytometry plot shows expression of TNF-α (I, J) and IFN-γ (K, L) expression CD3<sup>+</sup> CD8<sup>+</sup> from the CNS of Allo-HCT mice treated with either antibiotics or vehicle.

## Microbiome depletion upregulates p38 MAPK and NF-κB pathways in microglia

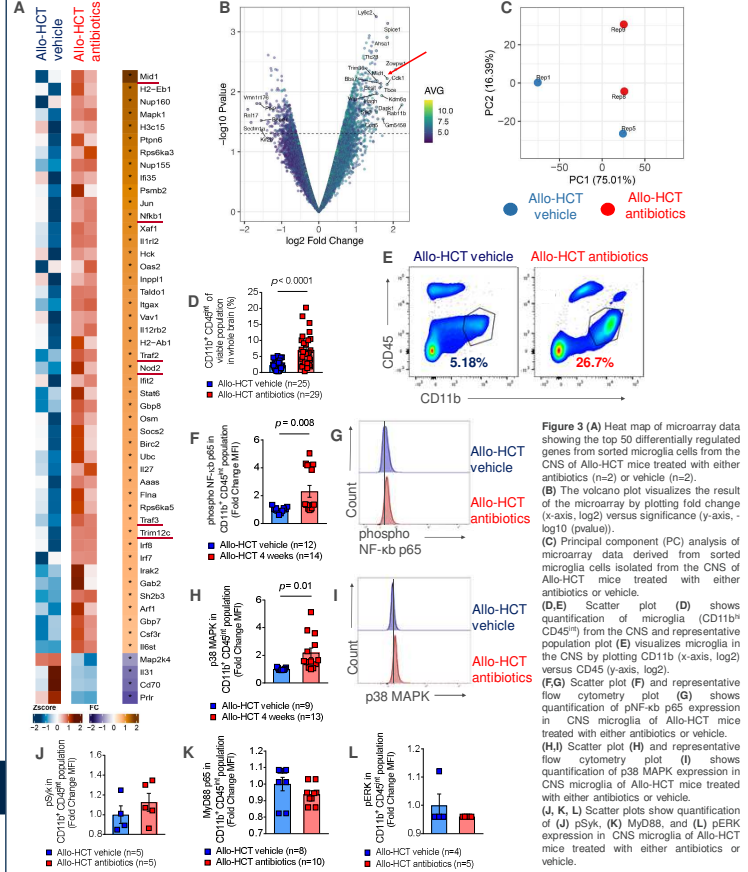


Figure 3 (A) Heat map of microarray data showing the top 50 differentially regulated genes from sorted microglia cells from the CNS of Allo-HCT mice treated with either antibiotics (n=2) or vehicle (n=2). (B) The volcano plot visualizes the result of the microarray by plotting log<sub>2</sub> fold change (x-axis, log<sub>2</sub>) versus significance (y-axis, -log<sub>10</sub> (p-value)). (C) Principal component (PC) analysis of microarray data derived from sorted microglia cells isolated from the CNS of Allo-HCT mice treated with either antibiotics or vehicle. (D, E) Scatter plot (D) shows quantification of microglia (CD11b<sup>+</sup> CD45<sup>+</sup>) from the CNS and representative population plot (E) visualizes microglia in the CNS by plotting CD11b (x-axis, log<sub>2</sub>) versus CD45 (y-axis, log<sub>2</sub>). (F) Scatter plot (F) and representative flow cytometry plot (G) shows quantification of p38 MAPK expression in CNS microglia of Allo-HCT mice treated with either antibiotics or vehicle. (H, I) Scatter plot (H) and representative flow cytometry plot (I) shows quantification of p38 MAPK expression in CNS microglia of Allo-HCT mice treated with either antibiotics or vehicle.

## Microbiome depletion upregulates activation markers on microglia

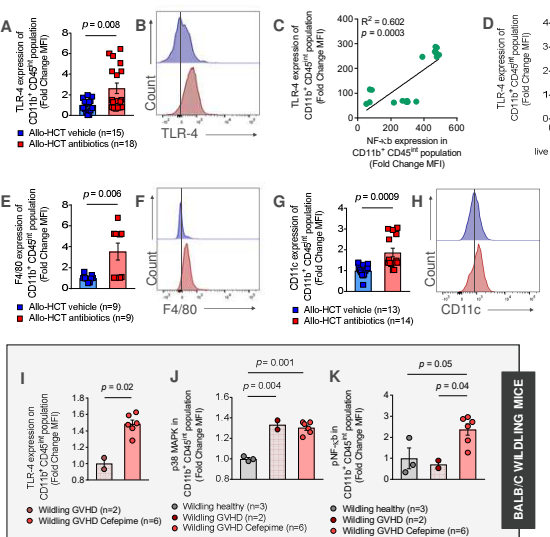


Figure 4 (A, B) Scatter plot (A) and representative flow cytometry plot (B) shows quantification of TLR4 expression on CNS microglia of Allo-HCT mice treated with either antibiotics or vehicle. (C, D) Scatter plots show correlation of TLR4 expression in CNS microglia and with (C) pNF-κB p65 expression in CNS microglia and with (D) quantification (percentage of total viable population) of T-cells (CD3<sup>+</sup> CD45<sup>+</sup>) in the CNS of Allo-HCT mice treated with either antibiotics or vehicle. (E, F) Scatter plot (E) and representative flow cytometry plot (F) shows quantification of F4/80 expression on CNS microglia of Allo-HCT mice treated with either antibiotics or vehicle. (G, H) Scatter plot (G) and representative flow cytometry plot (H) shows quantification of CD11c expression on CNS microglia of Allo-HCT mice treated with either antibiotics or vehicle. (I, J, K) Scatter plots show quantification of (I) TLR4, (J) p38 MAPK and (K) pNF-κB p65 expression in CNS microglia of healthy wildtype mice and Allo-HCT wildtype mice treated with celestipime or vehicle.

## Microbiome depletion worsens GVHD severity

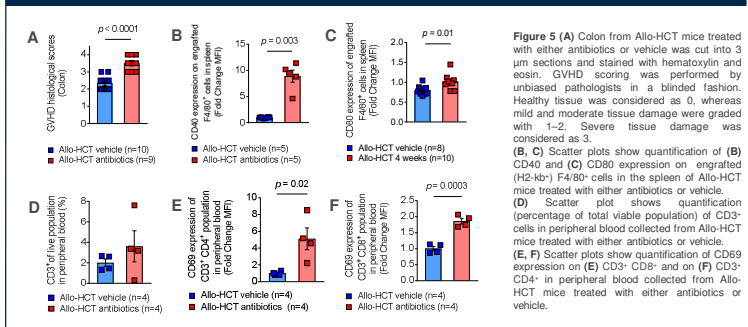


Figure 5 (A) Colon from Allo-HCT mice treated with either antibiotics or vehicle was cut into 3 μm sections and stained with hematoxylin and eosin. GVHD scoring was performed by unbiased pathologists in a blinded fashion. Healthy tissue was considered as 0, whereas mild and moderate tissue damage were graded with 1-2. Severe tissue damage was considered as 3. (B, C) Scatter plots show quantification of (B) CD40 and (C) CD80 expression on engrafted (H2-kg<sup>+</sup>) F4/80<sup>+</sup> cells in the spleen of Allo-HCT mice treated with either antibiotics or vehicle. (D) Scatter plot shows quantification (percentage of total viable population) of CD3<sup>+</sup> CD4<sup>+</sup> cells in peripheral blood collected from Allo-HCT mice treated with either antibiotics or vehicle. (E, F) Scatter plots show quantification of CD69 expression on (E) CD3<sup>+</sup> CD8<sup>+</sup> and on (F) CD3<sup>+</sup> CD4<sup>+</sup> in peripheral blood collected from Allo-HCT mice treated with either antibiotics or vehicle.

## References

- Mathew NR, Vinnakota JM et al. *Journal of Clinical Investigation*, 2019
- Erny D et al. *Nature Neuroscience*, 2015
- Zeiser R and Blazar BR. *New England Journal of Medicine*, 2017

Contact : Sangya Chatterjee- [sangya.chatterjee@uniklinik-freiburg.de](mailto:sangya.chatterjee@uniklinik-freiburg.de)